Supramolecular Self-Assembly of π-Conjugated Hydrocarbons *via* 2D Cooperative CH/π Interaction

Qing Li,[†,⊥] Chengbo Han,[‡,⊥] Scott R. Horton,[†] Miguel Fuentes-Cabrera,[†,§,*] Bobby G. Sumpter,[†,§] Wenchang Lu,[‡,§] Jerry Bernholc,[‡,§] Petro Maksymovych,[†,*] and Minghu Pan[†,*]

[†]Center for Nanophase Materials Sciences, Oak Ridge National Laboratory, Tennessee 37831, United States, [‡]Center for High Performance Simulation and Department of Physics, North Carolina State University, Raleigh, North Carolina 27695, United States, and [§]Computer Science and Mathematics Division, Oak Ridge National Laboratory, Tennessee 37831, United States. [⊥]These authors contributed equally to this work.

ABSTRACT

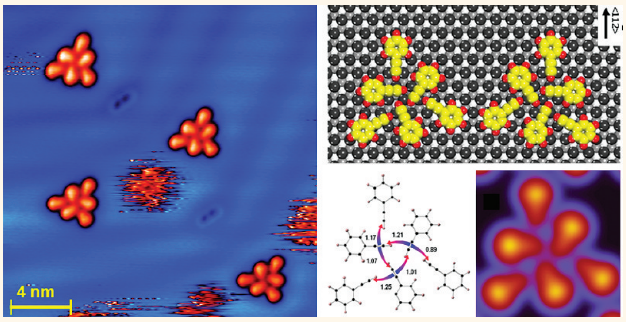

Supramolecular self-assembly on well-defined surfaces provides access to a multitude of nanoscale architectures, including clusters of distinct symmetry and size. The driving forces underlying supramolecular structures generally involve both graphoepitaxy and weak directional nonconvalent interactions. Here we show that functionalizing a benzene molecule with an ethyne group introduces attractive interactions in a 2D geometry, which would otherwise be dominated by intermolecular repulsion. Furthermore, the attractive interactions enable supramolecular self-assembly, wherein a subtle balance between very weak CH/π bonding and molecule-surface interactions produces a well-defined "magic" dimension and chirality of supramolecular clusters. The nature of the process is corroborated by extensive scanning tunneling microscopy/spectroscopy (STM/S) measurements and *ab initio* calculations, which emphasize the cooperative, multicenter characters of the CH/π interaction. This work points out new possibilities for chemical functionalization of π-conjugated hydrocarbon molecules that may allow for the rational design of supramolecular clusters with a desired shape and size.

KEYWORDS: phenylacetylene · self-assembly · STM · supramolecule · hydrogen bonding · magic cluster

One of the outstanding paradigms of nanoscience[1] is that of "magic" nanoparticles or molecular assemblies. For example, single atoms may aggregate into a cluster with a well-defined shape and size due to favorable saturation of the electronic shell in a particular "magic" atomic configuration.[2] Likewise, organic molecules can be self-assembled into magic clusters if there exists a structure that saturates the coordination shells of the constituent molecules bonded *via* specific interactions.[3−5] Weak directional molecular forces are central to self-assembly in general, and are particularly important for the formation of supramolecular structures on surfaces because they provide a balance between intermolecular and molecule-surface interactions, as well as the propensity toward coordination shell saturation.

Of the candidate attractive interactions, hydrogen bonding is by far the most significant. Typically, supra- and extended molecular structures are produced by functionalizing target molecules with strongly polar groups (such as OH, COOH, NO_2 *etc.*), and the ensuing hydrogen bonding (enthalpy varying from 3 to 7 kcal/mol).[6,7] However, electrons in C−C π-bonds, particularly those of the triple bond, can also act as a soft base and form the so-called XH/π hydrogen bond (X=O, N and halogen) with a comparatively smaller enthalpy, such as, from 2 to 4 kcal/mol.[8] In some special cases, the carbon atom itself can act as a soft acid leading to CH/π hydrogen bonds[9,10] with an enthalpy varying from 0.5 to 2 kcal/mol (the weakest of the hydrogen bonds). The potential advantage of CH/π bonding is its directionality (the CH fragment aligns perpendicular to the π orbital in a single CH/π bond) and the highly cooperative nature due to the ability of the CH/π fragments to act as both a Lewis acid and base.

Here we present a combined theoretical and experimental study that explores the possibility of utilizing weak CH/π bonding to enable 2D supramolecular self-assembly of flat-lying π-conjugated molecules. The latter, for example, benzene and pentacene, have long been a basic model system for an organic-metal interface which is key to a

* Address correspondence to
panm@ornl.gov,
fuentescabma@ornl.gov,
maksymovychp@ornl.gov.

Received for review October 13, 2011
and accepted December 14, 2011.

10.1021/nn203952e

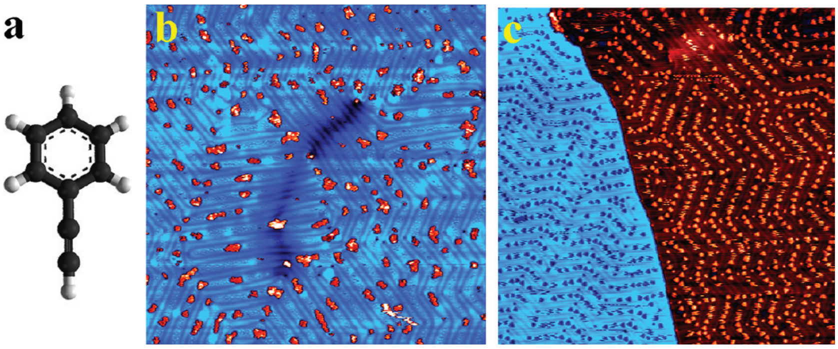

Figure 1. Topographic STM images of phenylacetylene molecules on Au(111), as-grown and after postannealing: (a) molecular structure of phenylacetylene; (b) phenylacetylene molecules form clusters after low temperature deposition at 50 K (800 mV, 30 pA), image size = 130 × 130 nm^2; (c) molecules self-assembled to form magic clusters array after annealing at 120 K (1 V, 30 pA), images size = 160 × 160 nm^2.

variety of electronic and energy-related applications. CH-π bonding between aromatic molecules on surfaces has been implicated previously, but so far primarily in 3D molecular assemblies,[11,12] where phenyl rings can orient normal or close to normal to each other. However, a parallel relative orientation of the π-conjugated system in the 2D geometry results in repulsive intermolecular interactions, preventing significant ordering within the molecular layer up to a relatively high coverage.[13,14] We will show that invoking ethyne groups as a source of attractive intermolecular interactions can solve this problem and enable supramolecular self-assembly in a 2D geometry.

RESULTS AND DISCUSSION

After low temperature deposition of ~0.1 ML, the phenylacetylene molecules (Figure 1a) clustered into largely disordered structures within the fcc domains of the Au(111) surface (Figure 1b). The height of a single molecular layer was around 0.15 nm, typical for flat-lying π-conjugated molecules.[13,15] Supramolecular self-assembly of regular clusters was triggered by postannealing the sample to ~120 K for 10 min, wherein most of the molecules on the surface rearranged themselves into a single type of cluster with a regular triangular shape and exactly six constituent phenylacetylene molecules (in the following we refer to this cluster as a hexamer). Increasing the coverage up to 0.3 ML only produced more hexamers, but neither their shape nor their internal structure changed (Figure 1c). The highly preferential formation of hexamers in a broad range of surface coverage (see Supporting Information, Figure S1) signifies the existence of "magic" rules that underpin supramolecular self-assembly of phenylacetylene on Au(111) (see Supporting Information, Figures S2 and S3).

Within the hexamer, one can differentiate three central molecules forming a pinwheel arrangement with ~120° relative angle between molecular axes, and three corner molecules each at ~90° angle with respect to its central neighbor (Figure 2a). The central pinwheel has a 3-fold symmetry axis but no mirror planes perpendicular to the surface, which gives rise to chirality. We schematically label this chirality as either a clockwise (C) or anticlockwise (A) orientation of the hexamer (see Figure 2a). From inspection of a large number of hexamers, we established that all A (and C) hexamers are oriented exactly the same way with respect to the surface. Equivalently, each complex can rotate only by 120°, and no other angle. Furthermore, the "axis" of each hexamer is rotated by approximately ±9° relative to the $\langle 11\bar{2}\rangle$ direction of the Au surface (Figure 2b,c). If we assume that the all phenylacetylene molecules within the hexamer occupy approximately the same surface site, it is straightforward to verify that there exists only one way to arrange the hexamer over the Au(111) surface that would satisfy the above spatial constraints. The corresponding structure is schematically shown in Figure 2a, where all the phenyl rings of the constituent molecules were positioned over the fcc-hollow sites and the hexamer became centered approximately around an atop surface site.

The involvement of CH/π bond in the stabilization of the hexamer is evident from the relative orientation of the ethyne groups within the hexamer, specifically the 90° angle between each corner molecule and its central neighbor, anticipated for CH/π bonding.[9] The structure of the hexamer also suggests that the phenyls rings do not contribute to the CH/π bonds. This is due to the surface parallel orientation of the π-conjugated phenyl ring, which prevents CH/π attractive interactions between the flat-lying phenyls. Notably, the relative angles between central molecules within the pinwheel are 120°.

To gain further insight into the hexamer's structure and the bonding mechanism, a hexamer was placed on a slab of Au(111) and relaxed using Density Functional Theory (DFT) calculations, with the PBE[16] functional and long-range interactions accounted for by the van der Waals (vdW)-DF approach.[17] The relaxed structure of the hexamer on Au(111) is shown in Figure 3b, and it is in very good agreement with

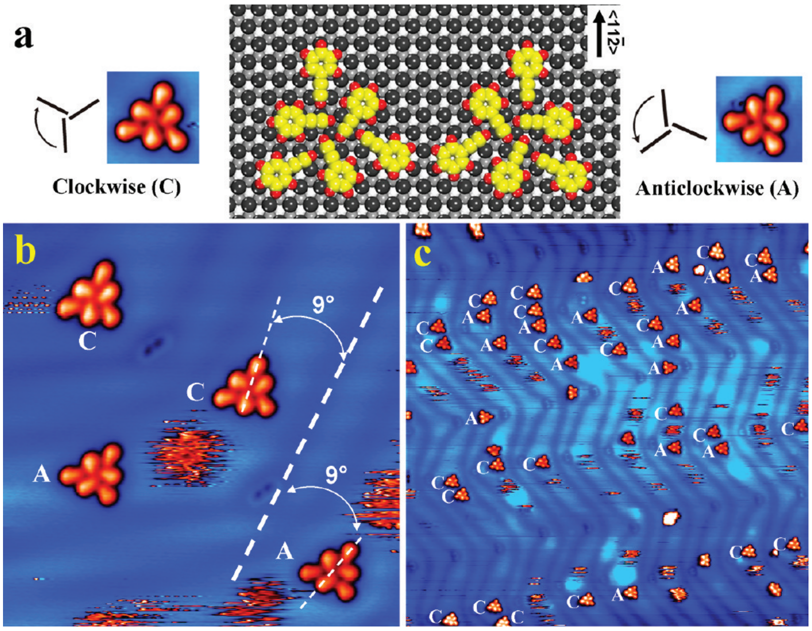

Figure 2. Chirality of the hexamer: (a) structural models showing the inferred adsorption configuration of hexamers with clockwise (C) and anticlockwise (A) chirality, mirrored with respect to $\langle 11\bar{2}\rangle$ direction of the Au(111) substrate. Enlarged STM images show the individual hexamer. (b) High resolution STM image showing few hexamers with both C and A chiralities (600 mV, 50 pA). White dashed line indicates the soliton line ($\langle 11\bar{2}\rangle$ crystallographic direction). Image size: 20 × 20 nm^2. (c) More hexamers in a larger area scan (800 mV, 30 pA), 60 × 60 nm^2.

the experimental observation: its size (the average distance between the centers of two corner molecules) is 16.4 Å, very close to the experimental value of 15.8 ± 0.5 Å; the average length of the CH/π bonds in the relaxed hexamer is 2.76 Å, in the upper range of bond lengths known from bulk experiments;[18] and the simulated scanning tunneling microscopy (STM) image (Figure 3c) with a sample bias of 800 meV agrees well with the experiment (Figure 3a).

The underlying bonding mechanism was investigated by performing a Natural Bond Orbital (NBO)[19] analysis for the relaxed structure of the hexamer. NBO analysis not only confirms the CH/π bonding, but also clearly emphasizes its cooperativeness (Figure 4): each central molecule acts as an electron acceptor for one of its central neighbors, and as an electron donor for one central and one corner neighbor. On the other hand, each corner molecule is only an electron acceptor from one of the central phenylacetylene molecules. In every case, the stabilization energy varies between 0.9 and 1.2 kcal/mol within the energy window of CH/π bonds (0.5−2 kcal/mol).

There remains a question of why six molecules is the "magic" number on Au(111). To address this question, we have computed the binding energies of gas-phase clusters comprising two, three, four, five, six, seven, and eight phenylacetylene molecules using PBE and vdW-DF (see Supporting Information, Figure S4a). In this case, the binding energies are defined as the energy gained by forming a cluster from isolated phenylacetylene molecules. We did not find a pronounced energy minimum for a hexamer (see Supporting Information, Figure S4b) and thus infer that the Au(111) substrate must play a crucial role in stabilizing the hexamer.

For starters, the hexamers are mostly located within the fcc domain of the herringbone reconstruction of the Au(111) surface. A similar phenomenon has been reported for many other molecules[20,21] on Au(111), and it can be understood on the basis of the domain dependence of the electronic potential[22] or, alternatively, the anisotropy of the adsorbate-induced stress.[23] However, we observe significant adsorption of both disordered and supramolecular clusters only within the fcc-region. Thus, we believe that the preference toward an fcc-stacked region cannot explain the stability of the hexamer.

A more relevant property is the epitaxial relationship of the hexamer relative to the surface lattice (Figure 2a), which has been inferred above from the statistics and relative orientation of the chiral supramolecular clusters. To probe the preferred adsorption site of the hexamer on the Au(111) surface, we have used *ab initio* techniques to calculate the binding energy of the hexamer in six different configurations, denoted here as fcc, top, hcp, bridge-hcp-fcc, bridge-hcp-top, and bridge-top-hcp (see Figure S5a in the Supporting Information for details). The binding energies were computed employing DFT with the PBE approximation to the exchange correlation potential, and the DFT-D2 approach of Grimme[24] to account for weak dispersion interactions. The results are shown in Figure 5b of the Supporting Information. The fcc adsorption site is most stable, followed by hcp at about

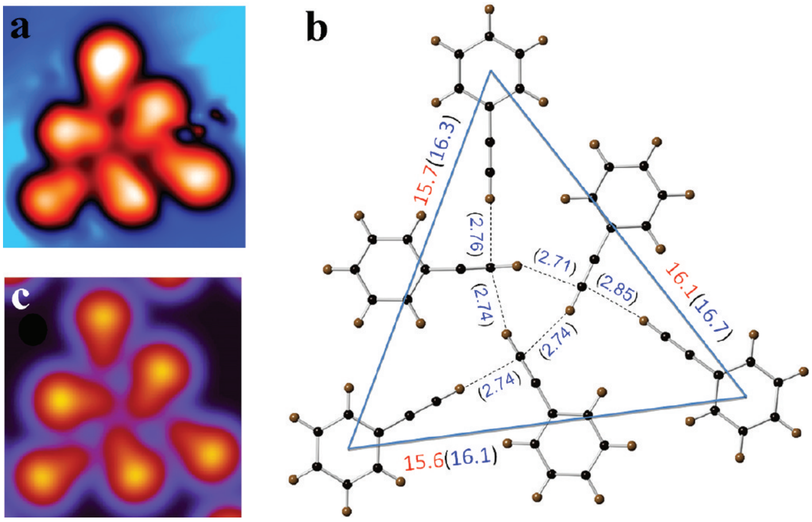

Figure 3. High-resolution STM image of a hexamer as well as its calculated structure. (a) High resolution STM image showing the internal structure of hexamer. (b) Structural model for the hexamer. Distances between the center of the rings of individual corner phenylacetylene molecules and the bonding lengths for each CH/π bonds are presented, in which experimental data are highlighted by red and calculated values are shown as blue numbers in brackets. (c) Theoretical simulated STM image for the fully relaxed hexamer on two layers of Au(111).

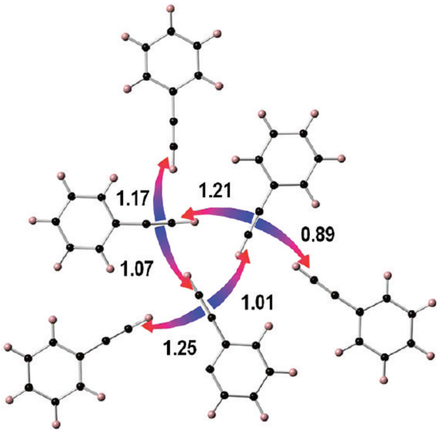

Figure 4. NBO analysis of the bonding motif for the relaxed hexamer. The arrows indicate the direction of electron transfer and the numbers above each arrow stand for the computed stabilization energy (in kcal/mol). The colors of each arrow indicate electron donor (blue) or electron acceptor (red) behavior.

47 meV apart. These results support the observation that there exists an epitaxial relationship between the molecules within the hexamer and the underlying lattice.

What happens if a seventh molecule is added to the hexamer in the 2D geometry? Maintaining a flat overall structure would make it necessary for the angle between this corner molecule and the bonded central partner, to deviate from 90°, in line with the 120° formed by cooperative CH/π bonding within the pinwheel center of the hexamer. Steric repulsion would clearly not favor this scenario, necessitating significant disruption of the center-corner CH/π bonding, and by extension of the other bonds within the hexamer. Furthermore, the seventh molecule would not be able to occupy the same surface site as its neighbors, and still avoid significant steric repulsion and optimize the CH/π bonding. Therefore, the hexamer is most likely the lowest-energy arrangement that satisfies three criteria: (1) maximum overall saturation of the coordination shell of the cooperative CH/π bonds; (2) 2D-geometry; and (3) favorable adsorption sites for all the constituent molecules. Although we do not have a fully conclusive answer to the origin of the "magic" rule at present, our findings immediately suggest that one should be able to form different supramolecular "magic" clusters by using different substrates.

The electronic properties of the hexamer were investigated by measuring the distance−voltage (Z−V) spectra,[25,26] which register displacement of the tip relative to the surface with increasing bias. When a resonance, such as a molecular state, falls into the tunneling window, an abrupt increase of the tunneling conductance takes place, which results in a step-like feature in the z-displacement curve (see Supporting Information, Figure S6). The numerically differentiated (dZ/dV) spectra acquired over a corner or central molecule are shown in Figure 5a. When the tip is placed over a corner molecule, a peak centered at ~3.32 V is registered, whereas a peak centered at ~3.21 V appears when the tip is placed over a central molecule. We argue that these peaks are associated with the collective lowest unoccupied molecular orbital (LUMO) state of the hexamer.

We computed the Projected Density of States (PDOS) of the hexamer placed on Au(111) surface by taking the sum of the PDOS for the phenyl rings over the hexamer (Figure 5b). Two peaks are observed and both have contributions from the corner and central molecules. This already implies that the LUMOs of the

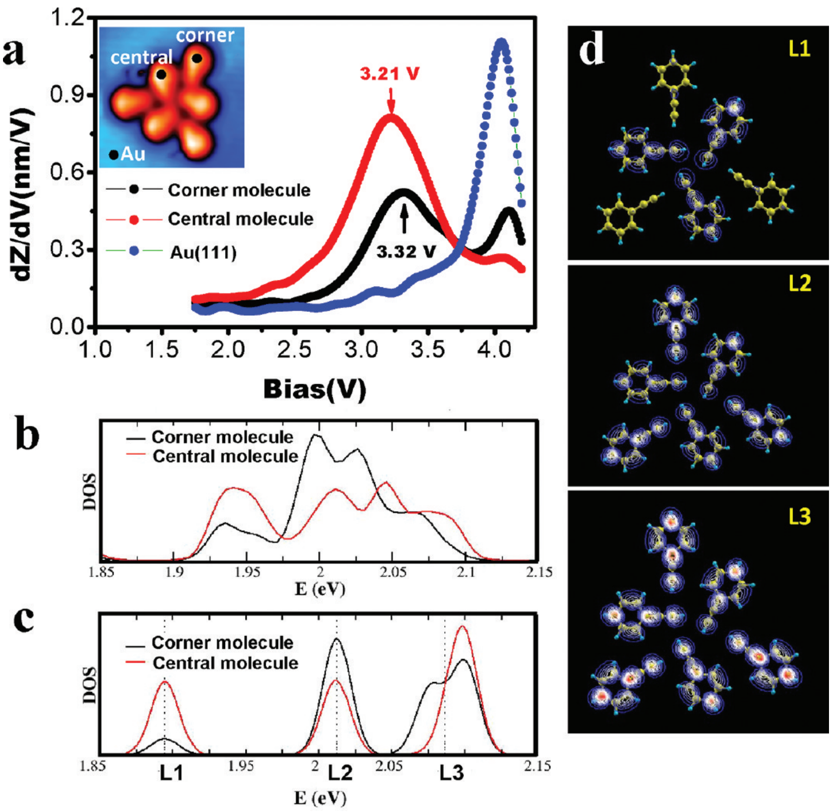

Figure 5. Electronic properties of a hexamer. (a) Numerically differentiated distance−voltage signal against the applied sample bias, d*Z*/d*V*, showing the LUMO states of the corner or central molecule in the hexamer. Inset figure shows locations of distance-voltage (*Z*−*V*) spectroscopic measurements over a corner, central molecule and bare Au surface, respectively. (b and c): *Ab-initio* projected density of states (PDOS) for the corner and central molecule sites in the hexamer on Au(111) and in the gas phase hexamer, respectively. The peaks L1, L2, and L3 in panel c correspond to the first six LUMO states of the hexamer. (d) Wave functions' moduli of the three peaks labeled in panel c.

parent molecules sufficiently hybridize and form several states split in energy. The peak below 2 eV has a larger weight on the central molecule, while the higher-energy peak has a majority component on a corner molecule. The calculated splitting is thus in qualitative agreement with the measured trend. The overlap of the constituent LUMO states is most clearly observed in the gas-phase PDOS calculations (Figure 5c,d), where three distinct energy levels are formed as a result of the overlap of LUMOs of the individual molecules.

CONCLUSIONS

We successfully synthesized uniform hexamers made of phenylacetylene molecules on a Au(111) surface. Both experiment and theory suggest that a balance between CH/π and surface−molecule interactions drives the favorable formation of the hexamers. Both the directionality and multicentricity of the CH/π bond appear to be critical for supramolecular self-assembly, dictating the number of molecules within the assembly and their relative orientation. It also appears that the substrate plays a significant role in defining the "magic" number six. Finally, *Z*−*V* spectroscopy has further revealed that the electronic properties of the molecules are modified upon self-assembly, specifically causing significant overlap of the LUMO states despite the relative weakness of the intermolecular interactions. We envision that adding more acetylene groups to the phenyl ring or using different substrates will allow for additional structural flexibility and possibly tunable control over the shape, size, and electronic properties of supramolecular assemblies, as well as the transition between supramolecular and extended self-assembled structures.

METHODS

Sample preparation and STM measurements were performed in an ultrahigh vacuum system (base pressure is better than 1×10^{-10} mbarr). Experiments were conducted with a home-built variable temperature scanning tunneling microscopy (VT-STM), whose temperature can vary from 25 to 300 K. In the present paper, if not otherwise mentioned, all the STM/S measurements are performed at 28 K. Phenylacetylene molecules were purified by the standard freeze−pump−thaw process. The Au(111) surface was cleaned by standard argon sputtering−annealing cycles before deposition of phenylacetylene molecules. The Au(111) substrate is kept at 50 K during the molecular deposition. A commercial Pt−Ir tip was carefully prepared by gentle field emission with clean Au(111) sample. The STM images were analyzed using WsXM.[27]

To compute the STM image, we first use PBE and vdW-DF to relax a hexamer on Au(111). We placed the hexamer structure on top of the Au surface in a position such that the center of each phenyl ring was positioned approximately above one of the Au atoms of the first layer. Two layers of gold were used to represent the Au(111) surface. The hexamer/Au(111) system was relaxed by keeping the Au atoms frozen and letting the hexamer relax fully. The calculations were done with the PWscf software[28] using an energy cutoff of 544 eV, a $2 \times 2 \times 1$ k-point mesh with a Gaussian smearing of 0.02 eV, and used dipole corrections.[29] The relaxation was carried out until all the forces in the hexamer were smaller than 0.001 Ry/a.u.

The NBO analysis was performed with the NWChem software[30] and employing PBE with the DFT-D2 approach and the 6-31G* basis set.

Relaxation of the clusters in gas-phase was performed using PBE and vdW-DF in a unit cell of dimensions 40 Å × 40 Å × 28.5 Å, which is large enough to avoid interaction between periodic images. The clusters were relaxed only in two dimensions, except for the $7'$ cluster, in which one phenylacetylene (the one in the plane perpendicular to that occupied by the hexamer) was allowed to relax in every direction.

The PDOS of the hexamer in gas-phase and on Au(111) was computed using PBE and vdW-DF.

Acknowledgment. This research was conducted at the Center for Nanophase Materials Sciences (CNMS), which is sponsored at Oak Ridge National Laboratory by the Office of Basic Energy Sciences, U.S. Department of Energy. The work at NCSU was supported by DOE Grant DE-FG02-98ER45685. The computations were performed using the resources of the CNMS and the National Center for Computational Sciences at Oak Ridge National Laboratory.

Supporting Information Available: (1) STM images show the coverage depended hexamer formation; (2) manipulation of the hexamers; (3) series of images show the stability of hexamers; (4) gas phase binding energy study with different cluster sizes; (5) binding energy of the hexamer in six different configurations on Au(111); (6) raw data of the *Z*/*V* spectra at different positions of the hexamer. This material is available free of charge *via* the Internet at http://pubs.acs.org.

REFERENCES AND NOTES

1. Bartels, L. Tailoring Molecular Layers at Metal Surfaces. *Nat. Chem.* **2010**, *2*, 87–95.
2. Heer, W. A. The Physics of Simple Metal Clusters: Experimental Aspects and Simple Models. *Rev. Mod. Phys.* **1993**, *65*, 611–676.
3. Yokoyama, T.; Yokoyama, S.; Kamikado, T.; Okuno, Y.; Mashiko, S. Selective Assembly on a Surface of Supramolecular Aggregates with Controlled Size and Shape. *Nature* **2001**, *413*, 619–621.
4. Bohringer, M.; Morgenstern, K.; Schneider, W. D.; Berndt, R.; Mauri, F.; Vita., A.; Car, R. Two Dimensional Self-Assembly of Supramolecular Clusters and Chains. *Phys. Rev. Lett.* **1999**, *83*, 324–327.
5. Heim, D.; Seufert, K.; Auwarter, W.; Aurisicchio, C.; Fabbro, C.; Bonifazi, D.; Barth, J. V. Suface-Assisted Assembly of Discrete Porphyrin-Based Cyclic Supramolecules. *Nano Lett.* **2010**, *10*, 122–128.
6. Pimentel, G. C.; McClellan, A. L. Hydrogen Bonding. *Annu. Rev. Phys. Chem.* **1971**, *22*, 347–385.
7. Weckesser, J.; Vita, A.; Barth, J. V.; Cai, C.; Kern, K. Mesoscopic Correlation of Supramolecular Chirality in One-Dimensional Hydrogen-Bonded Assemblies. *Phys. Rev. Lett.* **2001**, *87*, 096101−1–096101−4.
8. Desiraju, G. R.; Steiner, T. The Weak Hydrogen Bond in Structural Chemistry and Biology. Oxford University Press: Oxford, UK, 1999.
9. Nishio, M. CH/π Hydrogen Bonds in Crystals. *CrystEngComm* **2004**, *6*, 130–158.
10. Kumar, S.; Subramanian, K.; Srinivasan, R.; Rajagopalan, K.; Schreurs, A. M. M.; Kroon, J.; Steiner, T. *N*-(*p*-Methoxyphenyl)-*N*-prop-2-ynyl-urea: A Crystal Structure with the Rare Z'=5, and Statistical Data on Z' Values. *J. Mol. Struct.* **2000**, *520*, 131–139.
11. Torrente, I. F; Franke, K. J.; Henningsen, N.; Schulze, G.; Alemani, M.; Roth, Ch.; Rurali, R.; Lorente, N.; Pascual, J. I. Spontanous Formation of Triptycene Supramolecules on Surfaces. *J. Phys. Chem. B* **2006**, *110*, 20089–20092.
12. Pivetta, M.; Blüm, M. C.; Patthey, F.; Schneider, W. D. Two-Dimensional Tiling by Rubrene Molecules Self-Assembled in Supramolecular Pentagons, Hexagons, and Heptagons on a Au(111) Surface. *Angew. Chem., Int. Ed.* **2008**, *47*, 1076–1079.
13. Sykes, E. C. H.; Mantooth, B. A.; Han, P.; Donhauser, Z. J.; Weiss, P. S. Substrate-Mediated Intermolecular Interactions: A Quantitative Single Molecule Analysis. *J. Am. Chem. Soc.* **2005**, *126*, 7255–7260.
14. Dougherty, D. B.; Jin, W.; Cullen, W. G.; Reutt-Robey, J. E.; Robey, S. W. Variable Temperature Scanning Tunneling Microscopy of Pentacene Monolayer and Bilayer Phases on Ag(111). *J. Phys. Chem. C* **2008**, *112*, 20334–20339.
15. Han, P.; Mantooth, B. A.; Skyes, E. C. H.; Donhauser, Z. J.; Weiss, P. S. Benzene on Au(111) at 4 K: Monolayer Growth and Tip-Induced Molecular Cascades. *J. Am. Chem. Soc.* **2004**, *126*, 10787–10793.
16. Perdew, J. P.; Burke, K.; Ernzerhof, M. Generalized Gradient Approximation Made Simple. *Phys. Rev. Lett.* **1996**, *77*, 3865–3868.
17. Dion, M.; Rydberg, H.; Schroder, E.; Langreth, D. C.; Lundqvist, B. I. Van der waals Density Functional for General Geometries. *Phys. Rev. Lett.* **2004**, *92*, 246401−1−246401−4.
18. Steiner, T. Cooperative C≡C−H···C≡C−H Interaction: Crystal Structure of DL-Prop-2-ynylglycine and Database Study of Terminal Alkynes. *J. Chem. Soc., Chem. Commun.* **1995**, *1*, 95–96.
19. Reed, A. E.; Curtiss, L. A.; Weinhold, F. Intermolecular Interactions From a Natural Bond Orbital, Donor−Acceptor Viewpoint. *Chem. Rev.* **1988**, *88*, 899–926.
20. Cheng, Z. H.; Gao, L.; Deng, Z. T.; Jiang, N.; Liu, Q.; Shi, D. X.; Du, S. X.; Guo, H. M.; Gao, H. J. Adsorption Behavior of Iron Phthalocyanine on Au(111) Surface at Submonolayer Coverage. *J. Phys. Chem. C* **2007**, *111*, 9240–9244.
21. Ruffieux, P.; Palotás, K.; Gröning, O.; Wasserfallen, D.; Müllen, K.; Hofer, W. A.; Gröning, P.; Fasel, R. Site and Orientation-Selective Anchoring of a Prototypical Molecular Building Block. *J. Am. Chem. Soc.* **2007**, *129*, 5007–5011.
22. Chen, W.; Madhavan, V.; Jamneala, T.; Crommie, M. F. Scanning Tunneling Microscopy Observation of an Electronic Superlattice at the Surface of Clean Gold. *Phys. Rev. Lett.* **1998**, *80*, 1469–1473.
23. Haiss, W. Surface Stress of Clean and Adsorbate-Covered Solids. *Rep. Pro. Phys.* **2001**, *64*, 591–648.
24. Grimme, S. Semiempirical GGA-Type Density Functional Constructed with a Long-Range Dispersion Correction. *J. Comput. Chem.* **2006**, *27*, 1787–1799.
25. Dougherty, D. B.; Maksymovych, P.; Lee, J.; Yates, J. T. Local Spectroscopy of Image-Potential-Derived States: From Single Molecules to Monolayers of Benzene on Cu(111). *Phys. Rev. Lett.* **2006**, *97*, 236806−1–236806−4.
26. Feng, M.; Zhao, J.; Petek, H. Atomlike, Hollow-Core-Bound Molecular Orbitals of C60. *Science* **2008**, *320*, 359–362.
27. Horcas, I.; Fernandez, R.; Gomez-Rodriguez, J. M.; Colchero, J.; Gomez-Herrero, J.; Baro, A. M. WSXM: A Software for Scanning Probe Microscopy and a Tool for Nanotechnology. *Rev. Sci. Instrum.* **2007**, *78*, 013705−1–013705−8.
28. Giannozzi, P.; Baroni, P.; Bonini, N.; Calandra, M.; Car, R.; Cavazzoni, C.; Ceresoli, D.; Chiarotti, G. L.; Cococcioni, M.; Dabo, I.; *et al.* Quantum Espresso: A Modular and Open-Source Software Project for Quantum Simulations of Materials. *J. Phys-Condens. Mater.* **2009**, *21*, 395502−1–395502−19.

29. Bengtsson, L. Dipole Correction for Surface Supercell Calculations. *Phys. Rev. B* **1999**, *59*, 12301–12304.
30. Kendall, R. A.; Apra, E.; Bernholdt, D. E.; Bylaska, E. J.; Dupuis, M.; Fann, G. I.; Harrison, R. J.; Ju, J. L.; Nichols, J. A.; Nieplocha, J.; *et al*. High Performance Computational Chemistry: An Overview of NWChem a Distributed Parallel Application. *Comput. Phys. Commun.* **2000**, *128*, 260–283.